Terrain's steepness governs sensitivity of urban oak forests to climate variability

Yulia Prokopuk, Oleksandr Sylenko, Marcin Klisz, Annabel Porté, Maksym Netsvetov

Terrain's steepness governs sensitivity of urban oak forests to climate variability

Yulia Prokopuk[a,b,*], Oleksandr Sylenko[a,c], Marcin Klisz[b], Annabel Porté[d], Maksym Netsvetov[a,d]

[a]Institute for Evolutionary Ecology, National Academy of Sciences of Ukraine, 37, Academician Lebedev St, 03143, Kyiv, Ukraine

[b]Dendrolab IBL, Department of Silviculture and Genetics, Forest Research Institute, Raszyn, Poland

[c]Dendrological park «Olexandria» of NAS, Bila Tserkva-13, 09113, Ukraine

[d]BIOGECO, University of Bordeaux, INRAE, Cestas, France

*Corresponding author.

E-mail address: ju.prokopuk91@gmail.com (Y. Prokopuk).

Abstract. Urban forests, vital for providing ecosystem services in cities, face challenges from climatic factors, particularly in heterogeneous urban environments. Kyiv, one of Europe's largest and most populated cities, boasts a varied topography, with about 55% of its area covered by forests, where *Quercus robur* predominates. In this study we investigate the sensitivity of *Q. robur* trees to climatic factors within Kyiv's urban forest, utilizing tree ring widths as a proxy. Employing dendrochronological approaches, we built nine site-mean ring-width chronologies and identified the growth pointer years and their frequency. Using moving windows in daily correlation analysis, we examined *Q.robur* response to climatic variations

over the last 135 years. Additionally, linear mixed-effects models (LMMs) were applied to the site-specific characteristics such as slope steepness, altitude a.s.l., soil type, soil mechanical composition, soil pH, forest type and coefficient of soil saturated hydraulic conductivity, to identify which of them exert a significant influence on studied trees' sensitivity to precipitation and temperature. Our results showed that the frequency of negative or positive pointer years in *Q. robur* growth coincides with extremely dry or wet years. The precipitation amount falling from the dormant period to the early growing season emerges as the key factor for *Q. robur* trees' radial growth. The trees' sensitivity to this factor was found to be significantly influenced by the slope steepness. Our findings contribute valuable insights into the complex interplay between urban heterogeneity, climatic factors, and the climatic sensitivity of *Q. robur* in urban areas. This research contributes to a deeper understanding of urban forests' dynamics, proposing management strategies for slope stability, soil water retention, and natural tree regeneration.

Keywords: pedunculate oak, urban woodland, tree-ring width, slope, urban ecology

1. Introduction

Urban forests, comprising trees in streets, parks, gardens, and remnants of natural old-growth forests, provide a wide range of ecosystem services. These services include recreation, reduction of air pollution (Akbari, 2002; Nowak et al., 2018), carbon sequestration (Nowak and Crane, 2002), preservation of biodiversity (Alvey, 2006), protection against soil erosion, mitigation of rain water runoff

(Bartens et al., 2009), and improvement of urban climatic conditions through cooling and shading effect (Ellison et al., 2017; Lindén et al., 2016).

In general, the heterogeneity of the urban environment results in highly diverse microsite conditions influencing trees' functionality and viability, which can either weaken (Chen et al., 2011; Gillner et al., 2013) or strengthen (Schneider et al., 2022; Wilde and Maxwell, 2018) the climatic signals compared to nearby rural areas. Indeed, urban forests face significant stresses and disturbances particularly in comparison to suburban forests primarily due to human activities, forest fragmentation, and difference in local temperature and soil-water availability (Grimm et al., 2008; Wilde and Maxwell, 2018; Zhang and Brack, 2021). The heterogeneity of the city structure induces uneven temperatures in the cities and in particular, contributes to the formation of "heat islands"; this is leading to shifts in vegetation phenology (Li et al., 2019; Zhang and Brack, 2021) and alterations in tree-growth rates (Pretzsch et al., 2017). In addition, the effects of global climate change, such as temperature rising, precipitation redistribution in the season, and more frequent drought events have led to the decline of urban forests and an increased risk of trees mortality (Marchin et al., 2022; Romagnoli et al., 2018). Despite these challenges, individual trees might also benefit from urban conditions, in particular urban forest management and reduced competition for light (Wilde and Maxwell, 2018).

The local or site conditions have been shown to affect trees' growth and their responses to climate in forests in a broad ecological context (Klisz et al., 2023; Kostić et al., 2021; Lévesque et al., 2014; Ordóñez and Duinker, 2015). The local

hydrology, soil-water availability, and depth of soil water table are considered key that alter the climatic signal present in tree-growth series (Sass-Klaassen and Hanraets, 2006). Specific disturbances including soil compaction, root and crown damage etc. in the urban environment may also reduce trees' sensitivity to temperature and precipitations (Gillner et al., 2013; Helama et al., 2009), potentially lowering their ability to response to climate variations. In contrast, Schneider et al. (2022) reported that the presence of impervious surfaces and a high density of buildings in urban forests could increase trees' demand for soil moisture, thereby enhancing their climatic response. Therefore, the investigation of the local physical-chemical factors' influence on trees' growth-to-climate relationships can provide valuable insight into urban forest care.

In the field of dendrochronology, it has long been recognized that the sensitivity of trees to precipitation and drought can be influenced by the complex topography of their growth environment (Cook and Kairiukstis, 1990). Trees that grow on ridges and slopes capture stronger climatic signals compared to those at lower-lying sites (Fritts, 1976). This impact of topography on trees' climate sensitivity varies among species and is closely tied to their growth rate (Mayoral et al., 2019) and growth strategy (Fekedulegn et al., 2003). For instance, conservative species tend to be less sensitive to their position within the landscape, in contrast to site-specific and exploitative species (Fekedulegn et al., 2003). Meanwhile, topographic control on the climate sensitivity of trees' species can be quite prominent as well, particularly as it was found for *Quercus robur*, pedunculate oak, in steppe environments (Grytsan, 2000; Netsvetov et al., 2021). Trees in lower

positions may struggle with cold air drainage at the beginning of the growing season (Grytsan, 2000), leading to positive growth-to-temperature correlations that are not discernible in trees at higher sites (Netsvetov et al., 2021).

Our study aims to assess the sensitivity of *Q. robur*, a foundational species of European broadleaved forests, to climate variability and to identify the environmental factors contributing to the sensitivity of this species in urban areas. We hypothesize that this sensitivity is heterogeneous across all sites within the city, as the climatic signal is influenced by site-specific conditions, including topography, soil properties, and forest type. The magnitude and stability of *Q. robur'*s response to climatic factors, such as precipitation and temperature, are expected to vary depending on these local environmental conditions. To test this hypothesis, we analyzed ring-width chronologies from dominant and co-dominant *Q. robur* trees across nine urban forests in Kyiv, with varying habitat conditions, and used Linear Mixed-Effects Models (LMME) to evaluate the influence of these varying environmental factors on growth-climate relationships.

2. Materials and methods

2.1. Study sites

The study was performed in urban forests within Kyiv City, Ukraine. Although these forests were not situated immediately near buildings, they were frequently visited by city residents. The chosen nine study sites were characterized by the dominance of mature *Q. robur* trees, either in broadleaved forests or co-dominant in mixed forests (Fig. 1 and Table 1). Soil characteristics, including soil

type and mechanical composition, were obtained from the Soil Map of Ukraine, accessible on the European Soil Data Centre (Krupskyi et al., 1977), and interactive agricultural maps of Ukraine (Grachov, 2023). Topographic features were extracted from digital elevation models in QGIS (2024). Specifically, the average elevation (in meters above sea level) and slope (in degrees) of the studied sites were extracted. This allowed us to consider the impact of surface topography on microclimate and growth conditions.

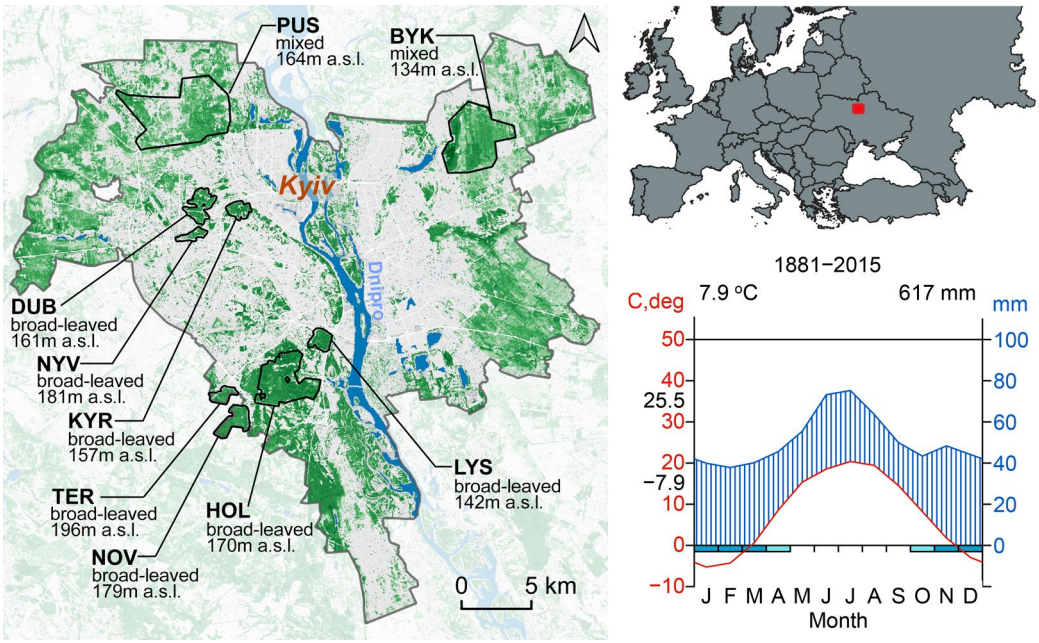

Fig. 1. The Kyiv city map with sampling sites (left), red square indicates the location of Kyiv city in Eastern Europe (top right panel) and Walter–Lieth climate diagram (bottom right panel)

The four studied sites namely Holosiivo (HOL), Novosilky (NOV), Teremky (TER), and Lysa Hora (LYS) represent old-growth oak-hornbeam forests located in the southern part of Kyiv, growing on light gray and gray podzolized soils. The origin of these forests remains debatable, however, the cartographic evidence and

130 the estimated age of some oak individuals suggest that a continuous forest massif
131 already existed in this area in the XVII century (Netsvetov and Prokopuk, 2016).
132 Altitudes range from 142 to 196 meters above sea level (m a.s.l.), and slopes vary
133 between 2.7 and 6.7 degrees at these sites (Table S1).

134

135 **Table 1**

136 Sampling sites description

Site ID	Lat. (°N)	Lon. (°E)	No. of trees/ cores	Age mean* (years)	$D_{1.3}$** mean± standard deviation (cm)	H**mean ± standard deviation (m)
HOL	50.359460	30.487721	32/64	227	106.3±20.04	23.9±3.03
NOV	50.343167	30.471227	19/44	164	89.6±10.23	24.0±1.57
TER	50.358710	30.446891	14/29	162	91.4±16.72	22.2±1.96
LYS	50.395951	30.550082	14/29	180	102.3±21.57	20.7±3.29
PUS	50.529865	30.383690	25/56	157	80.7±11.36	24.4±3.58
BYK	50.492626	30.685047	25/58	106	69.2±9.24	21.3±2.43
KYR	50.477596	30.469133	11/25	151	94.6±18.62	18.8±3.09
NYV	50.462650	30.423561	11/23	154	105.0±13.29	19.5±2.50
DUB	50.475405	30.421242	20/40	174	100.1±12.89	23.6±2.65

137 *The mean cambial age of the studied trees is given as of 2015

138 **Mean stem diameter at 1.3 m above ground level ($D_{1.3}$) and height (H) were
139 calculated from studied trees measurements

140

Pushcha Vodytsia (PUS) and Bykivnianskyi (BYK) sites are managed pine-oak forests in the northwest and northeast of the city, respectively, with soils classified as sod medium-podzolic loamy sand and sod weakly-podzolic sandy loam. These forests have been planted in areas that were originally covered by natural pine and pine-oak forests (Didukh and Aloshkina, 2012). The relief in most of this area is plain and the mean altitude ranges from 134 m in the BYK to 164 m a.s.l. in PUS (Table S1). Until the 1970s, the north and south parts of the city were sparsely built up.

The stands in Kyrylivskyi Hay Park (KYR), Dubky Park (DUB), and Nyvky Park (NYV) represent hornbeam-oak forests situated in the central part of Kyiv. The parks' stands are remnants of the typical deciduous forests that covered Kyiv's territory several centuries ago (Havryliuk and Rechmedin, 1956). The soils in these sites correspond to sod medium-podzolic loamy sand. The mean altitude varies from 157 m to 181 m a.s.l. and the terrain is characterized by ravines and beams with a mean slope of 4.1 to 6.8 degrees at these sites (Table S1).

2.2. Climatic data

The climate in the study area is moderately continental, with mild winters and warm summers. Over the study period of 1881–2015, the average annual air temperature in Kyiv was 7.9°C. Monthly mean temperatures varied from –7.9°C in January to 25.5°C in July. The average total annual precipitation value was 617 mm, with a maximal of 75 mm occurring in July, and a minimum of 38 mm in February (bottom-right plot at Fig. 1). In general, during the last decades climatic data show

a well-known rising temperature trend and no long-term change in precipitation in Kyiv (Netsvetov et al., 2018). The daily temperature and precipitation observations for the city were obtained from the European Climate Assessment dataset (Cornes et al., 2018).

2.3. Wood sampling

Wood samples were collected from visually healthy trees during autumn–winter seasons spanning 2015 to 2019. At sites where undamaged mature Q. robur trees were scarce, a minimum of 11 trees were sampled. A total of 171 dominant or co-dominant pedunculate oak trees were cored at breast height using 5 mm Haglöf increment borer. At least two increment cores per tree were collected. For each tree geographical coordinates were recorded and stem diameter at breast height and tree height were measured (Table 1).

2.4. Chronology development and pointer years analysis

Air-dried tree cores were prepared by affixing them to wooden supports, followed by successive sanding using increasingly fine-grained paper and high-resolution scanning at 3200 dpi using an Epson V37 scanner. Tree ring widths were measured with an accuracy of 0.01 mm utilizing the AxioVision (Carl Zeiss) software. Tree-ring widths series were cross-dated both within stems and among trees at each site using years of maximum and minimum growth as a benchmark.

To reduce non-climatic effects, we detrended the raw tree ring series using a cubic smoothing spline curve with a wavelength of 0.67 series duration (Cook and

Peters, 1981; Speer, 2010). Site-level residual chronologies of ring width indices (RWI) were built by calculating robust means for the standardized ring-width series prewhitened with a first-order autoregressive model (Cook and Kairiukstis, 1990). The chronologies cross-dating quality was checked with COFECHA software (Holmes, 1983) and the 'dplR' package (Bunn, 2010) in R (R Development Core Team, 2022).

For each site, we computed the standard deviation (SD) and the mean sensitivity (ms) to estimate the high-frequency variability of raw and detrended tree ring series. We also calculated the first-order autocorrelation coefficient (AR1) to identify relationships with previous growing season and the mean correlations between series from the same tree (rbar.wt) to estimate the quality of cross-dating for raw data; the mean correlation between trees (rbar.bt) for detrended chronologies. To assess chronologies' confidence, we computed the expressed population signal (EPS), the signal-to-noise ratio (snr), and the subsample signal strength (sss), using the 'dplR' package (Bunn, 2010) within R.

To identify years of extreme tree growth, both positive and negative deviations, we employed the bias-adjusted standardized growth change approach (BSGC) to the detrended tree ring series (Buras et al., 2022). The BSGC method also discerns the period of deflection, indicating the years when growth continued to deviate after an extreme event. In addition, we calculated the frequency of pointer years considering the BSGC results from all studied sites. This frequency (fi) was calculated using the formula:

$$fi = (ni / N-1)*100\%$$

where fi represents the frequency, ni is the number of sites with pointer years of the same sign, and N is the total number of studied sites. The determination of pointer years was proceeded using the 'dendRolAB' package (Buras et al., 2022) in R, focusing on the common period of detrended individual tree-ring series (1955–2015).

2.5. Trees' climate sensitivity assessment

To evaluate the sensitivity of *Q. robur* growth to climatic variables, we employed a double-moving window technique (Netsvetov et al., 2023; Prokopuk et al., 2022). The first window, spanning 31 years, was moved through the study period (1881–2015) in one-year steps. The second window analyzed daily climatic data using the daily_response function from the 'dendroTools' package in R (Jevšenak and Levanič, 2018). This method allowed us to identify the strongest correlations between tree growth and climate variables and to track the stability and duration of these relationships over time.

We applied the daily_response function 104 times for each site-specific tree-ring series: 104 times for temperature data and 104 times for precipitation data. This corresponds to the 104 overlapping 31-year windows within the study period. While there are technically 105 possible windows (105 = 2015 - 1881 +1- 31 + 1), the first year (1881) is used only to provide climatic conditions influencing tree growth in the following year (1882). This approach ensures that each window accounts for both current and previous season climatic influences, providing a comprehensive assessment of climate impacts on tree growth.

Each matrix generated by the daily_response function represents one 31-year window and one climatic variable (either temperature or precipitation). In these matrices, columns represent each day of the year, rows denote different window widths (in days), and cells contain the correlation coefficients between ring width time series and the 31-year period of daily climatic variables.

We then analyzed these 104 matrices for each combination of site chronology and climate variable using the Full-Duration at Half-Maximum (FDHM) method (Netsvetov et al., 2023; Weik, 2000). This method helps identify the most significant climate-to-growth patterns, focusing on peaks that exceed a 25% threshold to determine the duration and stability of these effects.

Additionally, we conducted the analysis using a fixed 1955–2015 window, which represents the common period for all individual chronologies. The results were then used to explore growth-climate relationships based on site characteristics (see the next chapter).

2.6. Linear mixed-effects models

We conducted linear mixed-effects models (LMM) to identify the local environmental variables influencing trees' growth and sensitivity to climate variations. We quantified trees' sensitivity to climate by considering the squared coefficient of correlation (R-squared) between RWI and climatic variables, i.e. temperature and precipitations. R-squared values were included in LMM as the response variable.

Physical-chemical characteristics of sites as well as forests types (Table S1) were tested as explanatory variables (fixed-effect parameters); sites IDs were included as a random-effect parameter. Fixed-effect parameters were progressively introduced in the initial restricted model, or null model, which initially contained only the random effect.

The best model was selected based on the corrected Akaike Information Criterion (AICc), and its effectiveness was compared with those of the null-model. Models with the AICc value lower than AICc of the null-model were considered to have the influence on trees' sensitivity to climate. The calculations were carried out using the 'lme4' package (Bates et al., 2015) in R.

2.7. Sensitivity to drought

The site-series sensitivity to drought was assessed employing the superposed epoch analysis SEA (Chree, 1913) implemented in the 'dplR' package in R (Bunn, 2010). Extreme drought events were identified based on years when the standardized precipitation-evapotranspiration index (SPEI) dropped to -2 or lower (McKee et al., 1993; Paulo et al., 2012). We focused on the SPEI1-SPEI6 indices, representing the aggregated interval from April to September, coinciding with the warmest period in the season and *Q. robur* wood formation (Lahoiko et al., 2019) (Fig. S3).

Subsequently, we used the mean ring width and RWI identified in SEA to assess the significance of their deviation from corresponding lag+1 years, i.e. randomly selected years served as a baseline to evaluate whether tree growth in drought years significantly deviated from mean growth. We then evaluated the

dependence of the deviation magnitude on the most influential factor identified in the LMM. Additionally, we utilized the maximum and minimum SPEI indices during the period of the *Q. robur* wood formation for a chi-squared test. This test enabled computation of the statistical significance of matches between the frequency of pointer years and extreme drought or wet events, SPEI <= - 2.0 and SPEI >= 2.0 respectively. All statistical analyses were conducted using R 3.6.3 (R Development Core Team, 2022).

3. Results

3.1. Chronology statistics

We established nine mean and residual tree-ring chronologies for the studied urban forests. The temporal span of these chronologies ranged from 152 years at the BYK and KYR sites to 259 years at the HOL site (Fig. 2, S1). The mean age of the trees across all sites in 2015 varied accordingly, from 106 years in BYK to 227 years in HOL (Table 1).

The age-related growth trend is evident across many trees (Fig. S1). Older trees, such as those found at HOL, exhibit lower growth rates, reflected in the corresponding mean ring width. During the study period from 1881 to 2015, the widest mean ring width was observed in BYK (2.93 ± 1.158 mm), while the narrowest was found in HOL (1.80 ± 0.591 mm) (Table 2).

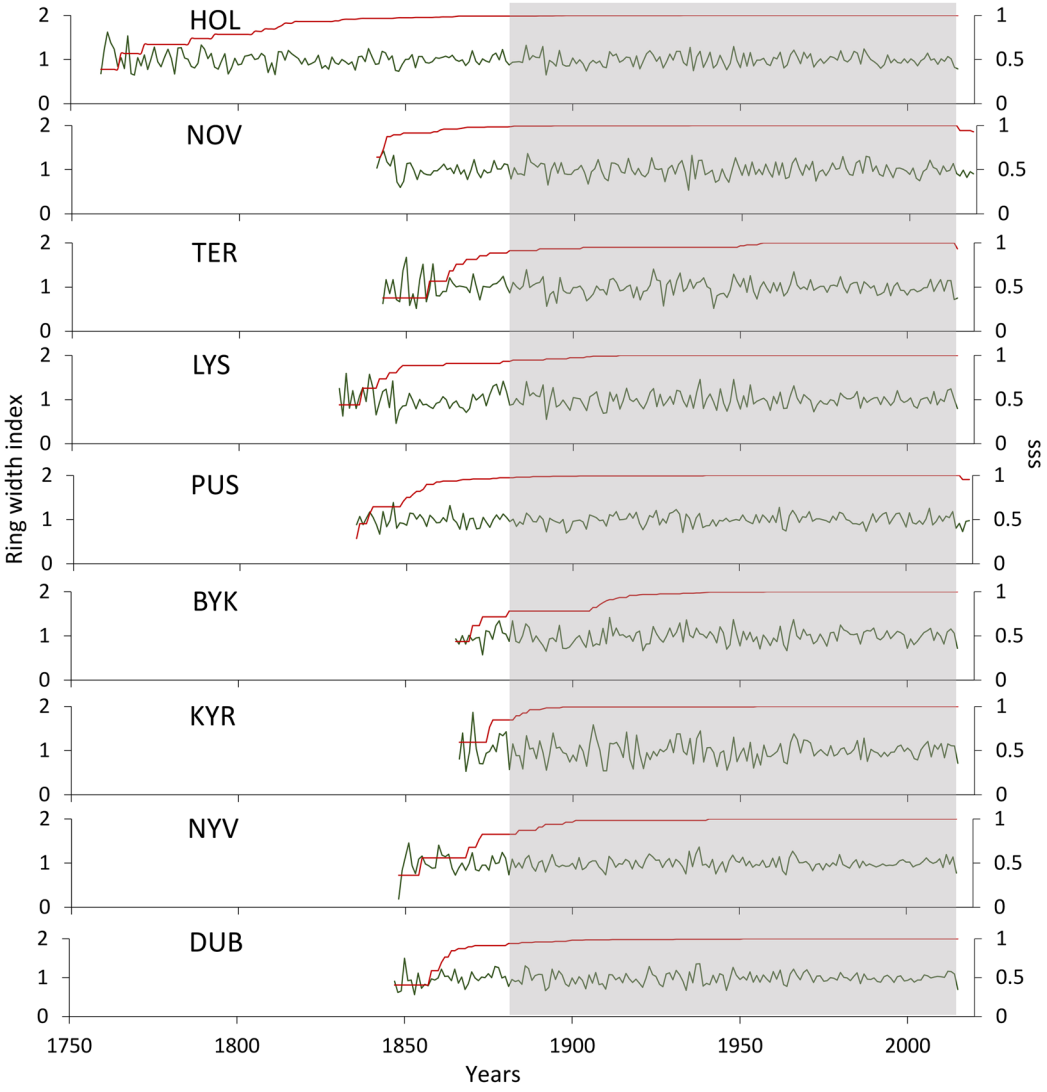

Fig. 2. Detrended chronologies (RWI) for each study site (see Table 1 for site ID code meaning). The red lines in the right panel indicate the subsample signal strength values and the shadowed rectangles point the studied period 1881–2015

Table 2

The chronologies descriptive statistics for the period 1881–2015

Site ID	MRW (mm)	SD (mm)	AR1	rbar.bt	rbar.wt	EPS	snr	sss	ms
HOL	1.80	0.591	0.688	0.388	0.666	0.952	19.9	>0.993	0.226
NOV	2.17	0.724	0.657	0.447	0.696	0.940	15.7	>0.989	0.248
TER	2.42	0.862	0.673	0.330	0.614	0.851	5.7	>0.911	0.246
LYS	2.26	0.991	0.728	0.402	0.691	0.899	8.8	>0.933	0.262
PUS	2.31	0.950	0.753	0.263	0.658	0.899	8.9	>0.975	0.247
BYK	2.93	1.158	0.720	0.414	0.684	0.928	12.9	>0.780	0.252
KYR	2.60	1.159	0.659	0.556	0.619	0.926	12.6	>0.847	0.299
NYV	2.55	0.911	0.730	0.298	0.572	0.811	4.3	>0.825	0.210
DUB	2.45	0.863	0.679	0.376	0.650	0.917	11.0	>0.941	0.237

MRW is the mean ring width, SD is the standard deviation, AR1 is the first-order autocorrelation coefficient, rbar.bt is the mean interseries correlation between all series from different trees, rbar.wt is the mean correlations between series from the same tree over all trees, EPS is the expressed population signal, snr is the signal-to-noise ratio, sss is the subsample signal strength, ms denotes the mean sensitivity. For site IDs, see Table 1.

A mixed-effects linear model revealed that forest types, most of soil properties, and topographical factors (see Table S1 and Table S2) did not have significant predictive capacity for tree growth variation. However, the model incorporating both soil mechanical composition and mean tree age demonstrated the best and only significant predictive performance for tree growth, explaining about 31% of the total growth variation across sites, based on marginal R-squared.

The AR1 values, which represent the dependence of the current year's growth on the previous year's growth, ranged from 0.66 at PUS to 0.75 at NOV. This indicates a significant degree of growth consistency across all studied forests, with NOV showing the strongest year-to-year dependence.

The rbar.bt varied across sites, with the highest value recorded at KYR (0.56), suggesting a more consistent growth response among trees at this site. Conversely, PUS exhibited the lowest correlation (0.26), indicating greater growth variability between individual trees. The rbar.wt values ranged from 0.60 at NYV to 0.71 at BYK, indicating a moderate level of correlation within trees across all sites.

The snr, a measure of the strength of the environmental signal in the tree-ring data, was highest at HOL (19.9) and lowest at NYV (4.3). This suggests that the HOL site has a much stronger, more consistent environmental influence on tree growth compared to the NYV site.

The lowest ms, which reflects the year-to-year growth variability, was recorded at NYV (0.21), suggesting relatively stable environmental conditions. In contrast, KYR exhibited the highest sensitivity (0.30), implying a greater responsiveness of trees to climatic variations.

EPS values, which measure the strength of the common signal across trees at each site or the representativeness of the sampled trees, exceeded 0.85 in all chronologies except for NYV (EPS = 0.81). Similarly, the subsample signal strength (sss) exceeded 0.85 in all sites except BYK (sss = 0.78) and NYV (sss = 0.83), indicating that these two sites may have more variability in the tree-ring signals or weaker sample coherence.

340

341 *3.2. Pointer years' analysis*

342 Using BSGC method on detrended tree-ring chronologies, we identified
343 negative and positive pointer years, as well as deflected periods, especially in recent
344 years (Fig. S2). Specific years stood out as notably unfavorable for tree growth,
345 including 1963, 1964 and 2015, when negative pointer years or deflected periods
346 were detected almost in all studied forests (Fig. S3). In contrast, 1966 and 1980 were
347 years in which tree growth significantly increased at most locations. Growth
348 depression was observed only in 1 to 4 sites, in 1956 (BYK, and KYR), 1959 (LYS),
349 1972 (HOL, NOV, LYS, and NYV), 1986 (LYS, KYR, and DUB), 1988 (PUS),
350 1992 (TER), 2002 (NOV), and 2014 (HOL, and TER). In contrast, growth release
351 was observed at some sites, in 1960 (NOV, and DUB), 1962 (PUS, BYK, NYV, and
352 DUB), 1969 and 1984 (HOL), 1987 (HOL, NOV, and KYR), 1997 (LYS), 2001
353 (PUS), 2006 (NOV), 2007 (TER, and PUS), 2008 (LYS), and 2012 (LYS, and
354 NYV).

355

356 *3.3. Climatic sensitivity of Quercus robur*

357 The use of a 31-year-wide moving window in daily partial correlation analysis
358 allowed us to establish a temporal stability pattern of climate sensitivity of *Q. robur*
359 in urban forests. A site-specific precipitation signal for oak chronologies was
360 corroborated. Specifically, trees in KYR, NYV, DUB, and HOL sites showed long-
361 term patterns of precipitation sensitivity that occurred from the dormant period to

362 early growing season (Figs. 3, S4 and Table 3). In contrast, on LYS and NOV sites,
363 the precipitation signal was prominent but not during the recent decades. Finally, in
364 TER, PUS, and BYK sites, trees displayed a weak or shifting relationship with
365 precipitation variability.

366 Moreover, in nearly all studied sites, the response of trees growth to
367 temperature was unstable for the overall study period (Figs. 3 and S5). The
368 correlation between growth and temperature inverted, shifting from positive to
369 negative in all study sites over the study period. Nevertheless, our analysis revealed
370 that high temperature reduced growth in the second half of the studied period in
371 HOL, NOV, and NYV, or during recent decades in TER, LYS, and DUB. Notably,
372 only BYK showed a relatively stable temperature- growth pattern, albeit interrupted
373 in several short periods.

374

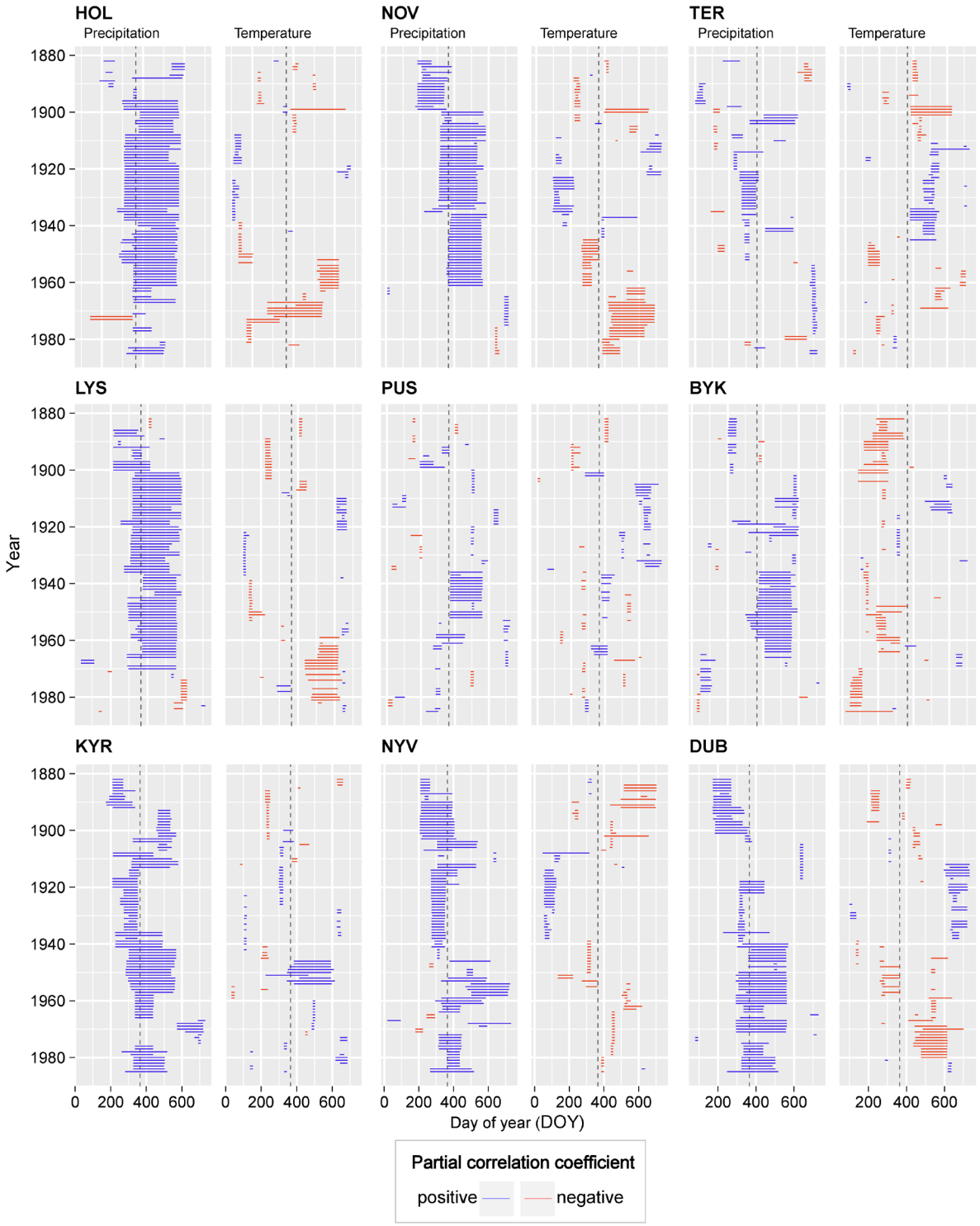

375

376 **Fig. 3.** Temporal changes in climate relationships across study period (vertical
377 dashed lines indicate the crossing between the previous and current year) per site:
378 left panel, with precipitations, right panel with temperature. Horizontal lines
379 represent the duration of the climatic predictors of growth within each 31-year time
380 window. The labels on the vertical axes are the first years of each time windows.
381 For site IDs, see Table 1

The calculated percentage of the strongest pattern of *Q. robur* climate-growth relationship revealed that the most stable positive correlation with precipitation varied from 26 % (TER) to 74 % (HOL) during the study period (Table 3, Fig. S4). The application of FDHM exhibited the most prominent patterns of positive correlation with precipitation, which occurred from the autumn of the previous year to the summer of the current season. An exception was TER site where only precipitation of the current year had a positive impact on *Q. robur* growth (Fig. S4). In contrast, the most stable negative temperature impact on *Q. robur* growth was identified from 13.5 % (TER) to 39.4 % (BYK) of all negative temperature correlations. The strongest temperature signal was revealed in BYK and NYV exhibited negative patterns, while TER showed a positive one (Fig. S4).

Table 3

Duration and percentage of the strongest patterns of climate-growth relationships. For site IDs, see Table 1.

Site ID	Precipitation positive			Precipitation negative			Temperature positive			Temperature negative		
	first DOY	last DOY	percent	first DOY	last DOY	percent	first DOY	last DOY	percent	first DOY	last DOY	percent
HOL	311	567	74.0	8	247	1.9	104	135	21.2	394	555	17.3
NOV	316	558	59.6	8	653	9.6	101	151	17.3	229	636	22.1
TER	689	699	26.0	107	130	8.7	458	527	27.9	133	571	13.5
LYS	310	557	69.2	406	592	9.6	612	658	19.2	422	618	17.3
PUS	373	559	30.8	6	400	6.7	377	668	19.2	199	396	15.4

BYK	370	569	38.5	28	42	6.7	103	570	10.6	190	2512	39.4
KYR	290	458	70.2	0	0	0	104	642	18.3	224	2455	21.2
NYV	270	406	62.5	181	284	3.9	55	111	23.1	304	5200	26
DUB	307	503	52.9	0	0	0	622	683	21.2	444	587	23.1

Among the various sites conditions and characteristics studied, terrain slope was the only factor that could be used as proxy of trees sensitivity to precipitations amount (Table 4), as revealed by the LMM modeling and AICc criterion comparisons. Meanwhile, for temperature sensitivity, no factor showed a higher predictive potential than the null model.

3.4. Sensitivity of trees to extreme drought

From 1955 to 2015, extreme droughts, as indicated by the SPEI1-6 index from April to September, were observed in Kyiv in 1959, 1964, 1975, 1979, 2001, 2002, 2009, 2010, and 2015. The negative slope of the regression line in the left plot of Fig. 4 demonstrates a negative relationship between terrain slope and mean ring width, indicating that as the slope increases, mean ring width tends to decrease. The R-squared value suggests that nearly 49% of the variability in mean ring width during drought years can be explained by the terrain's slope.

Similarly, the right plot in Fig. 4 shows a negative relationship between slope and standardized ring-width indices (RWI), indicating that trees on steeper slopes also experience reduced growth during drought, even after adjusting for baseline

growth trends. The R-squared value suggests that about 39% of the variability in standardized growth indices during droughts, as calculated in SEA, can be attributed to the terrain's slope.

Not all pointer years or deflected periods defined by the BSGC method matched with the seasonal dry or wet conditions expressed by SPEI (Fig. S3); however, a chi-squared test confirmed that the frequency of negative pointer years and extreme drought events, as well as the frequency of positive pointer years and extremely wet years, were not independent ($p < 0.05$). This indicates that significant tree growth anomalies, both positive and negative, are strongly associated with extreme climatic events, even though not every pointer year strictly coincides with an SPEI-defined drought or wet period.

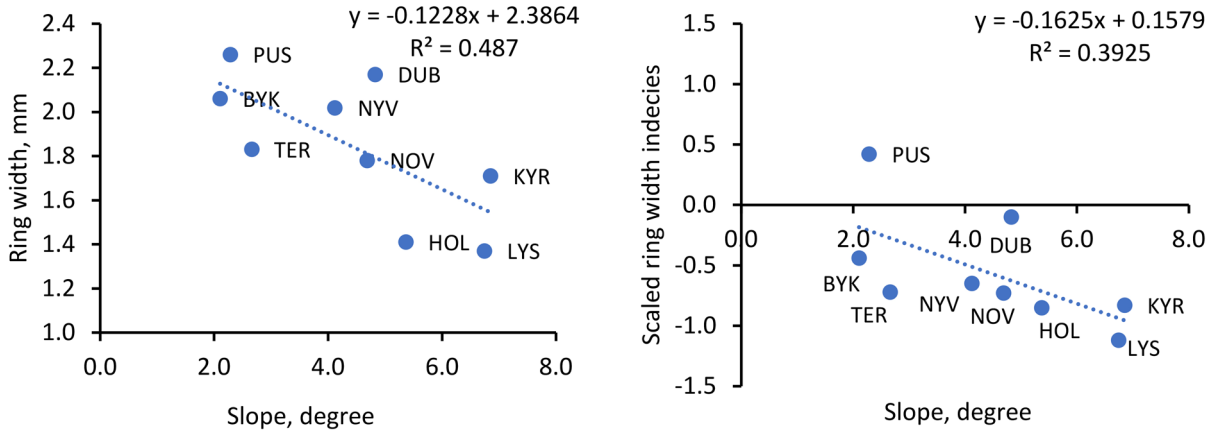

Fig. 4. The response of the mean ring width (left) and scaled RWI (right) on extreme droughts depending on site-mean slope. The dashed lines show linear regression. For site IDs, see Table 1

Table 4

Evaluation of the sites' characteristics determining urban forests sensitivity to precipitation and temperature. Linear mixed-effects models were used for assessing which factors were important in the trees' growth to climate relationship. The corrected second-order Akaike Information Criterion and the difference delta are presented. Bold characters indicate the model that performs better than the null model

Explanatory variables	Precipitation		Temperature	
	AICc	ΔAICc	AICc	ΔAICc
Null model	-448.4	0	-557.5	0
Slope	**-452.7**	**-4.3**	-556.2	1.3
Altitude	-448.0	0.4	-557.1	0.4
Soil type	-444.4	4.0	-552.3	5.2
Soil mechanical composition	-445.1	3.3	-554.5	3.0
Soil Ph	-446.6	1.8	-556.2	1.3
Forest type	-447.1	1.3	-555.7	1.8
Soil saturated hydraulic conductivity	-446.7	1.7	-555.7	1.8

The ecosystem services and benefits provided by urban forests are significantly influenced by tree dimensions, as larger trees have a greater potential for carbon sequestration, air quality improvement, and urban cooling (Mailloux et al., 2024; Prokopuk, 2019; Stephenson et al., 2014). In Kyiv, the radial growth rate of *Q. robur* is consistent with those reported in other urban and suburban forests

444 across Europe, including floodplain forests in Ukraine and Poland (Kalbarczyk et
445 al., 2018; Netsvetov et al., 2019, 2018), mixed forests in Latvia (Matisons et al.,
446 2013) and broadleaved forests in Moldova and Germany (Friedrichs et al., 2008;
447 Roibu et al., 2020; Scharnweber et al., 2011). This consistency suggests that *Q.*
448 *robur* can maintain a similar growth rate in diverse local environments within its
449 range in Central and Eastern Europe.

450 At the local scale, diverse conditions within the urban environment can either
451 facilitate or hinder tree growth. For instance, factors such as air pollution, soil
452 compaction, water availability, heat island effects, and proximity to infrastructure
453 can significantly influence growth patterns (Escobedo et al., 2011; Nechita et al.,
454 2021). Muscas et al. (2023) further emphasize that trees in park-like sites are less
455 impacted by urban stressors compared to those planted along streets, highlighting
456 the importance of less altered site-specific conditions for tree growth. Our findings
457 indicate that the mean tree age, combined with soil mechanical composition, are the
458 strongest predictors of the total growth variation of *Q. robur* in Kyiv. While the
459 influence of age on growth dynamics is well-known (Cook and Kairiukstis, 1990),
460 soil mechanical composition likely affects growth through its impact on water
461 retention, drainage capacity, and nutrient availability (Sheppard et al., 2001). Other
462 local factors, such as soil characteristics, were not significant predictors in our study,
463 possibly due to relatively low variability between sites or their covariation, which
464 may obscure their individual effects.

465 Tree growth in urban ecosystems is significantly impacted by severe drought
466 linked to climate change (Nitschke et al., 2017), and this is evident in the forests of

Kyiv, as highlighted by the pointer year analysis. Droughts were the primary driver of negative growth responses in *Q. robur* over the past five decades. The BSGC method identified 1963, 1964, and 2015 as negative pointer years, corresponding to periods of extreme droughts in Eastern Europe (Spinoni et al., 2015; Vicente-Serrano et al., 2010). In 2015, reduced tree ring widths were observed across all study sites, with significant growth depression recorded in seven of them (78%), coinciding with high summer temperatures and dry conditions that affected central-eastern Europe (Hoy et al., 2017).

In addition, the BSGC method identified 1966 as a positive pointer year in seven sites (78%) and 1980 in six sites (67%). The SPEI indices indicated "near-normal" moisture conditions in Kyiv during the 1966 growing season, which alone does not fully explain the simultaneous growth increase observed across the sites. This suggests that the growth surge may be a resilience response to the recurrent droughts experienced in previous years (Figs. S2 and S3). A similar pattern of increasing *Q. robur* growth after drought has been observed in the steppe region (Netsvetov et al., 2021). In 1980, the "very wet" spring and autumn conditions led to an increase in *Q. robur* growth (Fig. S3), pointing to the importance of water availability for the species' development in Kyiv's urban forests.

Site-specific conditions, whether natural or artificially altered, not only directly influence tree growth but also modulate their sensitivity to climatic factors, either mitigating or amplifying these effects. For instance, urban environments can enhance trees' responses to temperature fluctuations, particularly during summer heatwaves and in areas impacted by the urban heat island effect (Esperon-Rodriguez

et al., 2022; Schneider et al., 2022; Wilde and Maxwell, 2018). In natural forests at the southern margin of the species' range, the negative impact of high winter temperatures is exacerbated by local waterlogging conditions (García-González and Souto-Herrero, 2023). In contrast, in the steppe zone, convergent topographic position creates locally favorable conditions, making early-season temperatures beneficial for tree growth (Netsvetov et al., 2021).

In recent decades, a global reduction in the sensitivity of tree species to temperature, a divergence problem, has been observed and is attributed to the increasing impact of drought, pollution, micro-site conditions, and urban heat islands (Büntgen et al., 2009; Cook et al., 2004). This phenomenon is particularly pronounced in the Northern Hemisphere and has been registered in both coniferous species (Büntgen et al., 2006; Wilmking et al., 2005; Wilson et al., 2007) and deciduous species (Nechita et al., 2019). This trend is further supported by our findings in Kyiv's urban forests, where tree growth sensitivity to temperature appears inconsistent (see Fig. 3), although not significantly influenced by site conditions (Table 4).

However, in Kyiv, hillslope degree significantly influenced trees' radial growth sensitivity to precipitation, whereas other site characteristics, including soil type, had weaker predictive power than a null model. This finding contrasts with previous studies that identified local soil properties as the primary factor governing drought sensitivity in *Q. robur* (Buras et al., 2020; Kostić et al., 2021) and other species (Rehschuh et al., 2017; Rigling et al., 2001). The discrepancy could be attributed to the greater variability in soil types and fertility in these studies,

513 particularly in marginal southern populations where climate interacts with a diverse
514 range of soil conditions, from highly fertile to infertile soils (Kostić et al., 2021).

515 Another specificity in our findings is that while soil mechanical composition
516 explains growth rate variability across sites, it does not account for the effect of
517 precipitation. Soil mechanical composition determines baseline growth conditions
518 by influencing root development, nutrient availability, and aeration (Malamy, 2005),
519 thereby setting the potential growth rate of trees at each site. However, variations in
520 soil mechanical composition between sites may not fully explain differences in how
521 trees respond to short-term changes in precipitation. This may be particularly
522 relevant in landscapes with varied topography, such as hill slopes, where factors like
523 slope steepness and aspect have a strong influence on water runoff and retention,
524 thereby modulating tree sensitivity to precipitation (Hoylman et al., 2019).

525 Our results show that *Q. robur* sensitivity to precipitation variations and
526 extreme drought episodes increases with slope steepness (Fig. 4). In general, the
527 steeper the slope, the more pronounced the trees' sensitivity to water deficit. Trees
528 located on the highest and/or steepest slopes tend to exhibit enhanced drought
529 sensitivity or increased leaf defoliation, as observed in several broadleaved species,
530 including *Q. rubra* and *Q. prinus* (Hawthorne and Miniat, 2018) and *Q. ilex* (López-
531 Ballesteros et al., 2023). Slope, along with aspect, significantly influences
532 microclimate and hydrology by affecting factors such as vapor pressure deficit, wind
533 speed, radiation exposure, evaporative fluxes, cold air drainage, and overland water
534 flow (Thornthwaite, 1953;Gritsan, 2000; Sherratt, 2005; Dobrowsky, 2011;
535 Hoylman et al., 2019; Camarero et al., 2023). In our study, substantial variation in

aspect within sites precluded a detailed analysis of its effects, so we focused specifically on the influence of slope.

Steeper slopes limit soil-water recharge, leading to rapid surface water flow rather than infiltration into the soil (Gritsan, 2000; Dietrich and Perron, 2006). Additionally, surface water runoff contributes to erosion and the loss of topsoil (Hurst et al. 2012), thereby diminishing the soil's water retention capacity. Another crucial element related to slope is that shallow subsurface flow occurs less frequently and persistently on steeper slopes than on gentle slopes or at other topographic positions (Hoylman et al., 2019; Rempe and Dietrich, 2014).

Given *Q. robur*'s sensitivity to drought and the increasing frequency of drought episodes in Kyiv, integrating species distribution models into urban forest management policies is important. Based on the IPCC's climate projections under Shared Socioeconomic Pathways 485 and 245, as well as general circulation models (Dyderski et al., 2018; Puchałka et al., 2024), *Q. robur*'s natural distribution range is expected to shift northwards, with its southern boundary potentially moving towards the Kyiv region by 2060–2080. This projected range contraction underscores the need for proactive management strategies in Kyiv that prioritize slope stabilization and enhance water retention to mitigate soil erosion and ensure the long-term health and resilience of urban forests.

Our findings, along with insights from other studies, suggest several practical implications for managing urban forests under these changing conditions. Limiting public access to steep slopes can help reduce soil compaction and erosion caused by foot traffic, thereby preserving soil structure and improving water retention

(Buchwał and Rogowski, 2010; Matulewski, 2024). Establishing designated pathways for visitors, similar to those used in protected dune forests (Gouguet, 2018) and mountain forests (Barros et al., 2013), can effectively manage movement and reduce soil erosion on vulnerable slopes. These pathways are essential for maintaining natural hydrology and preventing the degradation of soil and vegetation.

In addition, minimizing intensive management activities on slopes, such as removal of organic debris, and instead leaving fallen branches and leaf litter on the forest floor, can reduce soil erosion and promote humus accumulation. This approach supports the natural regeneration process (Pemán et al., 2017), contributing to a more resilient urban forest ecosystem. Implementing soil conservation practices, such as mulching and maintaining native vegetation on slopes, can further enhance soil moisture retention and reduce surface runoff, thereby stabilizing the microclimate and increasing the soil's capacity to endure periods of water deficit.

Collectively, these practices will not only protect the health and stability of trees in city environments but also enhance the ecological integrity and aesthetic value of urban green spaces, aligning with the One Health concept (Prata et al., 2022) and contributing to public wellness and community resilience.

5. Conclusions

In this study, we evaluated the sensitivity of *Quercus robur* tree ring growth to climate in nine urban forests with distinct site-specific conditions in Kyiv city. The novelty of our study lies in demonstrating how slope steepness influences the climate sensitivity of urban forests. *Q. robur* trees are increasingly vulnerable to

582 climate changes, particularly on steeper slopes where water stress is heightened due
583 to rapid runoff and reduced soil moisture retention. This finding suggests that
584 management strategies should be optimized to account for both the tree species and
585 the specific topographic conditions.

586 Our study's practical implications for urban forestry management include
587 limiting public access to steep slopes, creating designated pathways to manage
588 visitor movement, and minimizing intensive management activities to promote
589 natural regeneration, help reduce the vulnerability of urban forests to climate-
590 induced stress, and maintain ecological stability in the face of changing climate
591 conditions.

592

593 **Funding**

594 This work is a part of scientific project of the National Academy of Sciences
595 of Ukraine to research laboratories/groups of young scientists (Code 6541230) 'The
596 impact of global climate change on the populations of individual plants and animals
597 world' (No. of state registration 0122U002153). This work has supported through
598 the MSCA4Ukraine project, which is funded by the European Union. Fellowship
599 Grant reference number: 1232738 (MN), 1233210 (YP).

600

601 **References**

602 Alvey, A.A., 2006. Promoting and preserving biodiversity in the urban forest. Urban
603 For Urban Green 5, 195–201. https://doi.org/10.1016/j.ufug.2006.09.003

604 Barros, A., Gonnet, J., Pickering, C., 2013. Impacts of informal trails on vegetation
605 and soils in the highest protected area in the Southern Hemisphere. J Environ
606 Manage 127, 50–60. https://doi.org/10.1016/j.jenvman.2013.04.030

607 Bartens, J., Day, S.D., Harris, J.R., Wynn, T.M., Dove, J.E., 2009. Transpiration and
608 Root Development of Urban Trees in Structural Soil Stormwater Reservoirs.
609 Environ Manage 44, 646–657. https://doi.org/10.1007/s00267-009-9366-9

610 Bates, D., Mächler, M., Bolker, B., Walker, S., 2015. Fitting Linear Mixed-Effects
611 Models Using **lme4**. J Stat Softw 67. https://doi.org/10.18637/jss.v067.i01

612 Buchwał, A., Rogowski, M., 2010. The methods of preventing trail erosion on the
613 examples of intensively used footpaths in the Tatra and the Babia Góra National
614 Parks. Geomorphologia Slovaca et Bohemica 1, 7–15.

615 Bunn, A.G., 2010. Statistical and visual crossdating in R using the dplR library.
616 Dendrochronologia (Verona) 28, 251–258.
617 https://doi.org/10.1016/j.dendro.2009.12.001

618 Büntgen, U., Frank, D.C., Schmidhalter, M., Neuwirth, B., Seifert, M., Esper, J.,
619 2006. Growth/climate response shift in a long subalpine spruce chronology.
620 Trees 20, 99–110. https://doi.org/10.1007/s00468-005-0017-3

621 Büntgen, U., Wilson, R., Wilmking, M., Niedzwiedz, T., Bräuning, A., 2009. The
622 "Divergence Problem" in tree-ring research, in: Tree Rings in Archaeology,
623 Climatology and Ecology. TRACE2008. Zakopane, Poland, pp. 212–219.

624 Buras, A., Ovenden, T., Rammig, A., Zang, C.S., 2022. Refining the standardized
625 growth change method for pointer year detection: Accounting for statistical bias
626 and estimating the deflection period. Dendrochronologia (Verona) 74, 125964.
627 https://doi.org/10.1016/j.dendro.2022.125964

628 Buras, A., Sass-Klaassen, U., Verbeek, I., Copini, P., 2020. Provenance selection
629 and site conditions determine growth performance of pedunculate oak.

630 Dendrochronologia (Verona) 61, 125705.
631 https://doi.org/10.1016/j.dendro.2020.125705

632 Camarero, J.J., Gazol, A., Valeriano, C., Pizarro, M., González de Andrés, E., 2023.
633 Topoclimatic modulation of growth and production of intra-annual density
634 fluctuations in Juniperus thurifera. Dendrochronologia (Verona) 82, 126145.
635 https://doi.org/10.1016/j.dendro.2023.126145

636 Chen, Z., He, X., Cui, M., Davi, N., Zhang, X., Chen, W., Sun, Y., 2011. The effect
637 of anthropogenic activities on the reduction of urban tree sensitivity to climatic
638 change: dendrochronological evidence from Chinese pine in Shenyang city.
639 Trees 25, 393–405. https://doi.org/10.1007/s00468-010-0514-x

640 Chree, C., 1913. Some phenomena of sunspots and of terrestrial magnetism at Kew
641 Observatory. Philosophical Transactions of the Royal Society of London. Series
642 A, Containing Papers of a Mathematical or Physical Character 212, 75–116.
643 https://doi.org/10.1098/rsta.1913.0003

644 Cook, E.R., Esper, J., D'Arrigo, R.D., 2004. Extra-tropical Northern Hemisphere
645 land temperature variability over the past 1000 years. Quat Sci Rev 23, 2063–
646 2074. https://doi.org/10.1016/j.quascirev.2004.08.013

647 Cook, E.R., Kairiukstis, L.A., 1990. Methods of dendrochronology. Springer
648 Netherlands, Dordrecht.

649 Cook, E.R., Peters, K., 1981. The smoothing spline: a new approach to standardizing
650 forest interior tree-ring width series for dendroclimatic studies. Tree-Ring
651 Bulletin 41, 45–53.

652 Cornes, R.C., van der Schrier, G., van den Besselaar, E.J.M., Jones, P.D., 2018. An
653 Ensemble Version of the E-OBS Temperature and Precipitation Data Sets.
654 Journal of Geophysical Research: Atmospheres. 123, 9391–9409.
655 https://doi.org/10.1029/2017JD028200

656 Didukh, Ya.P., Aloshkina, U.M., 2012. Biotops of Kyiv. NaUKMA, Agrar Media
657 Group, Kyiv.

658 Dietrich, W.E., Perron, J.T., 2006. The search for a topographic signature of life.
659 Nature 439, 411–418. https://doi.org/10.1038/nature04452

660 Dobrowski, S.Z., 2011. A climatic basis for microrefugia: the influence of terrain on
661 climate. Glob Chang Biol 17, 1022–1035. https://doi.org/10.1111/j.1365-
662 2486.2010.02263.x

663 Dyderski, M.K., Paź, S., Frelich, L.E., Jagodziński, A.M., 2018. How much does
664 climate change threaten European forest tree species distributions? Glob Chang
665 Biol 24, 1150–1163. https://doi.org/10.1111/gcb.13925

666 Ellison, D., Morris, C.E., Locatelli, B., Sheil, D., Cohen, J., Murdiyarso, D.,
667 Gutierrez, V., Noordwijk, M. van, Creed, I.F., Pokorny, J., Gaveau, D.,
668 Spracklen, D. V., Tobella, A.B., Ilstedt, U., Teuling, A.J., Gebrehiwot, S.G.,
669 Sands, D.C., Muys, B., Verbist, B., Springgay, E., Sugandi, Y., Sullivan, C.A.,
670 2017. Trees, forests and water: Cool insights for a hot world. Global
671 Environmental Change 43, 51–61.
672 https://doi.org/10.1016/j.gloenvcha.2017.01.002

673 Escobedo, F.J., Kroeger, T., Wagner, J.E., 2011. Urban forests and pollution
674 mitigation: Analyzing ecosystem services and disservices. Environmental
675 Pollution 159, 2078–2087. https://doi.org/10.1016/j.envpol.2011.01.010

676 Esperon-Rodriguez, M., Tjoelker, M.G., Lenoir, J., Baumgartner, J.B., Beaumont,
677 L.J., Nipperess, D.A., Power, S.A., Richard, B., Rymer, P.D., Gallagher, R. V.,
678 2022. Climate change increases global risk to urban forests. Nat Clim Chang 12,
679 950–955. https://doi.org/10.1038/s41558-022-01465-8

680 Fekedulegn, D., Hicks, R.R., Colbert, J.J., 2003. Influence of topographic aspect,
681 precipitation and drought on radial growth of four major tree species in an
682 Appalachian watershed. For Ecol Manage 177, 409–425.
683 https://doi.org/10.1016/S0378-1127(02)00446-2

684 Friedrichs, D.A., Buntgen, U., Frank, D.C., Esper, J., Neuwirth, B., Loffler, J., 2008.
685 Complex climate controls on 20th century oak growth in Central-West
686 Germany. Tree Physiol 29, 39–51. https://doi.org/10.1093/treephys/tpn003

687 Fritts, H.C., 1976. Tree Rings and Climate. Elsevier. https://doi.org/10.1016/B978-
688 0-12-268450-0.X5001-0

689 García-González, I., Souto-Herrero, M., 2023. Earlywood anatomy highlights the
690 prevalent role of winter conditions on radial growth of oak at its distribution
691 boundary in NW Iberia. Plants 12, 1185.
692 https://doi.org/10.3390/plants12051185

693 Gillner, S., Vogt, J., Roloff, A., 2013. Climatic response and impacts of drought on
694 oaks at urban and forest sites. Urban For Urban Green 12, 597–605.
695 https://doi.org/10.1016/j.ufug.2013.05.003

696 Gouguet, L., 2018. Guide de gestion des dunes et des plages associées. éditions
697 Quae. https://doi.org/10.35690/978-2-7592-2482-1

698 Grachov, A., 2023. Soil map of Ukraine [WWW Document]. Maps of Ukraine.
699 Available at: https://geomap.land.kiev.ua/soil-6.html.

700 Grimm, N.B., Faeth, S.H., Golubiewski, N.E., Redman, C.L., Wu, J., Bai, X.,
701 Briggs, J.M., 2008. Global Change and the Ecology of Cities. Science (1979)
702 319, 756–760. https://doi.org/10.1126/science.1150195

703 Grytsan, Y.I., 2000. Ecological bases transformative impact of forest vegetation on
704 steppe environment (in Ukrainian). Dnipropetrovsk University Press,
705 Dnipropetrovsk.

706 Havryliuk, V.S., Rechmedin, I.O., 1956. Nature of Kyiv and its outskirts. Kyiv state
707 university of T.G.Shevchenka, Kyiv.

708 Hawthorne, S., Miniat, C.F., 2018. Topography may mitigate drought effects on
709 vegetation along a hillslope gradient. Ecohydrology 11.
710 https://doi.org/10.1002/eco.1825

711 Helama, S., Läänelaid, A., Raisio, J., Tuomenvirta, H., 2009. Oak decline in Helsinki
712 portrayed by tree-rings, climate and soil data. Plant Soil 319, 163–174.
713 https://doi.org/10.1007/s11104-008-9858-z

714 Holmes, R.L., 1983. Computer assisted quality control in tree-ring dating and
715 measurement.Tree-Ring Bull. Tree-Ring Bulletin 43, 69–78.

716 Hoy, A., Hänsel, S., Skalak, P., Ustrnul, Z., Bochníček, O., 2017. The extreme
717 European summer of 2015 in a long-term perspective. International Journal of
718 Climatology 37, 943–962. https://doi.org/10.1002/joc.4751

719 Hoylman, Z.H., Jencso, K.G., Hu, J., Holden, Z.A., Allred, B., Dobrowski, S.,
720 Robinson, N., Martin, J.T., Affleck, D., Seielstad, C., 2019. The Topographic
721 Signature of Ecosystem Climate Sensitivity in the Western United States.
722 Geophys Res Lett 46, 14508–14520. https://doi.org/10.1029/2019GL085546

723 Hurst, M.D., Mudd, S.M., Walcott, R., Attal, M., Yoo, K., 2012. Using hilltop
724 curvature to derive the spatial distribution of erosion rates. J Geophys Res Earth
725 Surf 117. https://doi.org/10.1029/2011JF002057

726 Jevšenak, J., Levanič, T., 2018. dendroTools: R package for studying linear and
727 nonlinear responses between tree-rings and daily environmental data.
728 Dendrochronologia (Verona) 48, 32–39.
729 https://doi.org/10.1016/j.dendro.2018.01.005

730 Kalbarczyk, R., Ziemiańska, M., Machowska-Molik, A., 2018.
731 Dendroclimatological Analysis of Radial Growth of Old-Growth Oak (Quercus
732 Robur L.) on the Oder River Floodbank in the City of Wrocław, South-Western
733 Poland. Drvna industrija 69, 149–161. https://doi.org/10.5552/drind.2018.1745

734 Klisz, M., Puchałka, R., Jakubowski, M., Koprowski, M., Netsvetov, M., Prokopuk,
735 Y., Jevšenak, J., 2023. Local site conditions reduce interspecific differences in
736 climate sensitivity between native and non-native pines. Agric For Meteorol
737 341, 109694. https://doi.org/10.1016/j.agrformet.2023.109694

738 Kostić, S., Wagner, W., Orlović, S., Levanič, T., Zlatanov, T., Goršić, E., Kesić, L.,
739 Matović, B., Tsvetanov, N., Stojanović, D.B., 2021. Different tree-ring width
740 sensitivities to satellite-based soil moisture from dry, moderate and wet
741 pedunculate oak (Quercus robur L.) stands across a southeastern distribution
742 margin. Science of The Total Environment 800, 149536.
743 https://doi.org/10.1016/j.scitotenv.2021.149536

744 Krupskyi, N., Voronina, A., Bohdanovych, V., 1977. Soil map of Ukraine [WWW
745 Document]. European soil data centre (ESDAC). Available at:
746 https://esdac.jrc.ec.europa.eu/content/title-russia-soil-map-ukraine.

747 Lahoiko, A., Prokopuk, Y., Netsvetov, M., 2019. Wood formation in two Quercus
748 robur phenological forms in Kyiv, Ukraine, in: Tree Rings in Archaeology,
749 Climatology and Ecology - TRACE 2019. San Leucio-Caserta, Italy, p. 147.

750 Lévesque, M., Rigling, A., Bugmann, H., Weber, P., Brang, P., 2014. Growth
751 response of five co-occurring conifers to drought across a wide climatic gradient
752 in Central Europe. Agric For Meteorol 197, 1–12.
753 https://doi.org/10.1016/j.agrformet.2014.06.001

754 Li, X., Rossi, S., Liang, E., 2019. The onset of xylogenesis in Smith fir is not related
755 to outer bark thickness. Am J Bot 106, 1386–1391.
756 https://doi.org/10.1002/ajb2.1360

757 Lindén, J., Fonti, P., Esper, J., 2016. Temporal variations in microclimate cooling
758 induced by urban trees in Mainz, Germany. Urban For Urban Green 20, 198–
759 209. https://doi.org/10.1016/j.ufug.2016.09.001

760 López-Ballesteros, A., Rodríguez-Caballero, E., Moreno, G., Escribano, P., Hereş,
761 A., Yuste, J.C., 2023. Topography modulates climate sensitivity of multidecadal
762 trends of holm oak decline. Glob Chang Biol 29, 6336–6349.
763 https://doi.org/10.1111/gcb.16927

764 Mailloux, B.J., McGillis, C., Maenza-Gmelch, T., Culligan, P.J., He, M.Z., Kaspi,
765 G., Miley, M., Komita-Moussa, E., Sanchez, T.R., Steiger, E., Zhao, H., Cook,

766 E.M., 2024. Large-scale determinants of street tree growth rates across an urban
767 environment. PLoS One 19, e0304447.
768 https://doi.org/10.1371/journal.pone.0304447

769 Malamy, J.E., 2005. Intrinsic and environmental response pathways that regulate
770 root system architecture. Plant Cell Environ 28, 67–77.
771 https://doi.org/10.1111/j.1365-3040.2005.01306.x

772 Marchin, R.M., Esperon-Rodriguez, M., Tjoelker, M.G., Ellsworth, D.S., 2022.
773 Crown dieback and mortality of urban trees linked to heatwaves during extreme
774 drought. Science of The Total Environment 850, 157915.
775 https://doi.org/10.1016/j.scitotenv.2022.157915

776 Matisons, R., Elferts, D., Brūmelis, G., 2013. Pointer years in tree-ring width and
777 earlywood-vessel area time series of Quercus robur—Relation with climate
778 factors near its northern distribution limit. Dendrochronologia (Verona) 31,
779 129–139. https://doi.org/10.1016/j.dendro.2012.10.001

780 Matulewski, P., 2024. Scots pine roots (Pinus sylvestris L.) as
781 dendrogeomorphological indicators of soil erosion on a hiking trail in the
782 Brodnica Lakeland, Poland NE. Catena (Amst) 245, 108316.
783 https://doi.org/10.1016/j.catena.2024.108316

784 Mayoral, C., van Breugel, M., Turner, B.L., Asner, G.P., Vaughn, N.R., Hall, J.S.,
785 2019. Effect of microsite quality and species composition on tree growth: A
786 semi-empirical modeling approach. For Ecol Manage 432, 534–545.
787 https://doi.org/10.1016/j.foreco.2018.09.047

788 McKee, T.B., Nolan, J., Kleist, J., 1993. The relationship of drought frequency and
789 duration to time scales, in: Proceedings of the 8th Conference on Applied
790 Climatology, Anaheim, California, 17-22 January. pp. 179–183.

791 Muscas, D., Fornaciari, M., Proietti, C., Ruga, L., Orlandi, F., 2023. Tree growth
792 rate under urban limiting conditions. Eur J For Res 142, 1423–1437.
793 https://doi.org/10.1007/s10342-023-01599-0

794 Nechita, C., Čufar, K., Macovei, I., Popa, I., Badea, O.N., 2019. Testing three
795 climate datasets for dendroclimatological studies of oaks in the South
796 Carpathians. Science of The Total Environment 694, 133730.
797 https://doi.org/10.1016/j.scitotenv.2019.133730

798 Nechita, C., Iordache, A.M., Lemr, K., Levanič, T., Pluhacek, T., 2021. Evidence of
799 declining trees resilience under long term heavy metal stress combined with
800 climate change heating. J Clean Prod 317, 128428.
801 https://doi.org/10.1016/j.jclepro.2021.128428

802 Netsvetov, M., Prokopuk, Y., Didukh, Y., Romenskyy, M., 2018. Climatic
803 sensitivity of Quercus robur L. in floodplain near Kyiv under river regulation.
804 Dendrobiology 79, 20–33. https://doi.org/10.12657/denbio.079.003

805 Netsvetov, M., Prokopuk, Y., Holiaka, D., Klisz, M., Porté, A.J., Puchałka, R.,
806 Romenskyy, M., 2023. Is there Chornobyl nuclear accident signature in Scots
807 pine radial growth and its climate sensitivity? Science of The Total Environment
808 878, 163132. https://doi.org/10.1016/j.scitotenv.2023.163132

809 Netsvetov, M., Prokopuk, Y., Ivanko, I., Kotovych, O., Romenskyy, M., 2021.
810 Quercus robur survival at the rear edge in steppe: Dendrochronological
811 evidence. Dendrochronologia (Verona) 67, 125843.
812 https://doi.org/10.1016/j.dendro.2021.125843

813 Netsvetov, M., Prokopuk, Y., Puchałka, R., Koprowski, M., Klisz, M., Romenskyy,
814 M., 2019. River Regulation Causes Rapid Changes in Relationships Between
815 Floodplain Oak Growth and Environmental Variables. Front Plant Sci 10.
816 https://doi.org/10.3389/fpls.2019.00096

817 Netsvetov, M.V., Prokopuk, Yu.S., 2016. Age and radial growth of age-old trees of
818 Quercus robur in Feofania Park. Ukrainian Botanical Journal 73, 126–133.
819 https://doi.org/10.15407/ukrbotj73.02.126

820 Nitschke, C.R., Nichols, S., Allen, K., Dobbs, C., Livesley, S.J., Baker, P.J., Lynch,
821 Y., 2017. The influence of climate and drought on urban tree growth in southeast

822 Australia and the implications for future growth under climate change. Landsc
823 Urban Plan 167, 275–287. https://doi.org/10.1016/j.landurbplan.2017.06.012

824 Ordóñez, C., Duinker, P.N., 2015. Climate change vulnerability assessment of the
825 urban forest in three Canadian cities. Clim Change 131, 531–543.
826 https://doi.org/10.1007/s10584-015-1394-2

827 Paulo, A.A., Rosa, R.D., Pereira, L.S., 2012. Climate trends and behaviour of
828 drought indices based on precipitation and evapotranspiration in Portugal.
829 Natural Hazards and Earth System Sciences 12, 1481–1491.
830 https://doi.org/10.5194/nhess-12-1481-2012

831 Pemán, J., Chirino, E., Espelta, J.M., Jacobs, D.F., Martín-Gómez, P., Navarro-
832 Cerrillo, R., Oliet, J.A., Vilagrosa, A., Villar-Salvador, P., Gil-Pelegrín, E.,
833 2017. Physiological keys for natural and artificial regeneration of oaks. pp. 453–
834 511. https://doi.org/10.1007/978-3-319-69099-5_14

835 Prata, J.C., Ribeiro, A.I., Rocha-Santos, T., 2022. An introduction to the concept of
836 One Health, in: One Health. Elsevier, pp. 1–31. https://doi.org/10.1016/B978-
837 0-12-822794-7.00004-6

838 Pretzsch, H., Biber, P., Uhl, E., Dahlhausen, J., Schütze, G., Perkins, D., Rötzer, T.,
839 Caldentey, J., Koike, T., Con, T. van, Chavanne, A., Toit, B. du, Foster, K.,
840 Lefer, B., 2017. Climate change accelerates growth of urban trees in
841 metropolises worldwide. Sci Rep 7, 15403. https://doi.org/10.1038/s41598-017-
842 14831-w

843 Prokopuk, Y., Leshcheniuk, O., Sukhomlyn, M., Matiashuk, R., Budzhak, V.,
844 Netsvetov, M., 2022. Growth drivers of monumental wild service tree (Sorbus
845 torminalis) out of its natural range in Kyiv, Ukraine. Dendrobiology 87, 163–
846 170. https://doi.org/10.12657/denbio.087.012

847 Prokopuk, Yu.S., 2019. Reconstruction of annual carbon sequestration in stems of
848 Quercus robur (Fagaceae) in the floodplain forests of Kyiv. Ukrainian Botanical
849 Journal 75, 517–524. https://doi.org/10.15407/ukrbotj75.06.517

Puchałka, R., Paź-Dyderska, S., Jagodziński, A.M., Sádlo, J., Vitková, M., Klisz, M., Nicolescu, V.-N., Koniakin, S., Prokopuk, Y., Netsvetov, M., Zlatanov, T., Dyderski, M.K., 2024. Predicted range shifts of the main forest forming trees in Europe, in: Chiatante, D., Devetaković, J. (Eds.), PEN-CAFoRR Final Conference. University of Belgrade – Faculty of Forestry, Kneza Višeslava 1, Belgrade, Serbia, Belgrade, pp. 70–71.

QGIS.org, 2024. QGIS Geographic Information System. Open Source Geospatial Foundation Project. [WWW Document]. URL http://qgis.org (accessed 8.31.24).

R Development Core Team, 2022. A language and environment for statistical computing.

Rehschuh, R., Mette, T., Menzel, A., Buras, A., 2017. Soil properties affect the drought susceptibility of Norway spruce. Dendrochronologia (Verona) 45, 81–89. https://doi.org/10.1016/j.dendro.2017.07.003

Rempe, D.M., Dietrich, W.E., 2014. A bottom-up control on fresh-bedrock topography under landscapes. Proceedings of the National Academy of Sciences 111, 6576–6581. https://doi.org/10.1073/pnas.1404763111

Rigling, A., Waldner, P.O., Forster, T., Bräker, O.U., Pouttu, A., 2001. Ecological interpretation of tree-ring width and intraannual density fluctuations in *Pinus sylvestris* on dry sites in the central Alps and Siberia. Canadian Journal of Forest Research 31, 18–31. https://doi.org/10.1139/x00-126

Roibu, C.-C., Sfeclă, V., Mursa, A., Ionita, M., Nagavciuc, V., Chiriloaei, F., Leșan, I., Popa, I., 2020. The Climatic Response of Tree Ring Width Components of Ash (Fraxinus excelsior L.) and Common Oak (Quercus robur L.) from Eastern Europe. Forests 11, 600. https://doi.org/10.3390/f11050600

Romagnoli, M., Moroni, S., Recanatesi, F., Salvati, R., Mugnozza, G.S., 2018. Climate factors and oak decline based on tree-ring analysis. A case study of peri-

877 urban forest in the Mediterranean area. Urban For Urban Green 34, 17–28.
878 https://doi.org/10.1016/j.ufug.2018.05.010

879 Sass-Klaassen, U., Hanraets, E., 2006. Woodlands of the past — The excavation of
880 wetland woods at Zwolle-Stadshagen (the Netherlands): Growth pattern and
881 population dynamics of oak and ash. Netherlands Journal of Geosciences -
882 Geologie en Mijnbouw 85, 61–71.
883 https://doi.org/10.1017/S0016774600021429

884 Scharnweber, T., Manthey, M., Criegee, C., Bauwe, A., Schröder, C., Wilmking,
885 M., 2011. Drought matters – Declining precipitation influences growth of Fagus
886 sylvatica L. and Quercus robur L. in north-eastern Germany. For Ecol Manage
887 262, 947–961. https://doi.org/10.1016/j.foreco.2011.05.026

888 Schneider, C., Neuwirth, B., Schneider, S., Balanzategui, D., Elsholz, S., Fenner, D.,
889 Meier, F., Heinrich, I., 2022. Using the dendro-climatological signal of urban
890 trees as a measure of urbanization and urban heat island. Urban Ecosyst 25, 849–
891 865. https://doi.org/10.1007/s11252-021-01196-2

892 Sheppard, P.R., Casals, P., Gutiérrez, E., 2001. Relationship between ring-width
893 variation and soil nutrient availability at the tree scale. Tree Ring Res 57, 105–
894 113.

895 Sherratt, J.A., 2005. An Analysis of Vegetation Stripe Formation in Semi-Arid
896 Landscapes. J Math Biol 51, 183–197. https://doi.org/10.1007/s00285-005-
897 0319-5

898 Speer, J.H., 2010. Fundamentals of tree ring research. University of Arizona Press,
899 Tucson.

900 Spinoni, J., Naumann, G., Vogt, J., Barbosa, P., 2015. European drought
901 climatologies and trends based on a multi-indicator approach. Glob Planet
902 Change 127, 50–57. https://doi.org/10.1016/j.gloplacha.2015.01.012

903 Stephenson, N.L., Das, A.J., Condit, R., Russo, S.E., Baker, P.J., Beckman, N.G.,
904 Coomes, D.A., Lines, E.R., Morris, W.K., Rüger, N., Álvarez, E., Blundo, C.,
905 Bunyavejchewin, S., Chuyong, G., Davies, S.J., Duque, Á., Ewango, C.N.,
906 Flores, O., Franklin, J.F., Grau, H.R., Hao, Z., Harmon, M.E., Hubbell, S.P.,
907 Kenfack, D., Lin, Y., Makana, J.-R., Malizia, A., Malizia, L.R., Pabst, R.J.,
908 Pongpattananurak, N., Su, S.-H., Sun, I.-F., Tan, S., Thomas, D., van Mantgem,
909 P.J., Wang, X., Wiser, S.K., Zavala, M.A., 2014. Rate of tree carbon
910 accumulation increases continuously with tree size. Nature 507, 90–93.
911 https://doi.org/10.1038/nature12914

912 Thornthwaite, C.W., 1953. A charter for climatology. World Meteorological
913 Organization Bulletin 2, 40–46.

914 Vicente-Serrano, S.M., Beguería, S., López-Moreno, J.I., 2010. A Multiscalar
915 Drought Index Sensitive to Global Warming: The Standardized Precipitation
916 Evapotranspiration Index. J Clim 23, 1696–1718.
917 https://doi.org/10.1175/2009JCLI2909.1

918 Weik, M.H., 2000. full-width at half-maximum, in: Computer Science and
919 Communications Dictionary. Springer US, Boston, MA, pp. 661–661.
920 https://doi.org/10.1007/1-4020-0613-6_7770

921 Wilde, E.M., Maxwell, J.T., 2018. Comparing climate-growth responses of urban
922 and non-urban forests using L. tulipifera tree-rings in southern Indiana, USA.
923 Urban For Urban Green 31, 103–108.
924 https://doi.org/10.1016/j.ufug.2018.01.003

925 Wilmking, M., D'Arrigo, R., Jacoby, G.C., Juday, G.P., 2005. Increased temperature
926 sensitivity and divergent growth trends in circumpolar boreal forests. Geophys
927 Res Lett 32. https://doi.org/10.1029/2005GL023331

928 Wilson, R., D'Arrigo, R., Buckley, B., Büntgen, U., Esper, J., Frank, D., Luckman,
929 B., Payette, S., Vose, R., Youngblut, D., 2007. A matter of divergence: Tracking
930 recent warming at hemispheric scales using tree ring data. Journal of

931 Geophysical Research: Atmospheres 112.
932 https://doi.org/10.1029/2006JD008318

933 Zhang, B., Brack, C.L., 2021. Urban forest responses to climate change: A case
934 study in Canberra. Urban For Urban Green 57, 126910.
935 https://doi.org/10.1016/j.ufug.2020.126910

936

Table S1

The site-specific characteristics of studied forests

Site ID	Slope mean ± standard deviation (degree)	Altitude mean ± standard deviation (m)	Soil type	Soil mechanical composition	Soil pH	Forest type	Soil saturated hydraulic conductivity (cm/s)
HOL	5.4± 3.96	170± 20.1	light gray and gray podzolized soils; dark gray podzolized soils	sandy	up to 4.5 extremely acidic	broadleaved	0.00051 moderetly high
NOV	4.7± 3.09	179± 11.9	light gray and gray podzolized soils; sod medium-podzolic loamy sand soils; sod mainly gleyed sandy, loamy-sandy and sandy soils with humous sands soils	sandy	up to 4.5 extremely acidic	broadleaved	0.00051 moderetly high
TER	2.7± 1.65	196± 3.3	light gray and gray podzolized soils; sod medium-podzolic loamy sand soils; sod mainly gleyed sandy, loamy-sandy and sandy soils with humous sands soils	sandy	up to 4.5 extremely acidic	broadleaved	0.00051 moderetly high
LYS	6.7± 4.62	142± 14.7	light gray and gray podzolized soils; dark gray	sandy	up to 4.5 extremely acidic	broadleaved	0.00051 moderetly high

			podzolized soils				
PUS	2.3± 1.54	164± 15.2	sod medium-podzolic loamy sand soils	loam-sandy	4.5-5.0 very strong acidic	mixed	0.00051 moderetly high
BYK	2.1± 1.55	134± 17.6	sod medium-podzolic loamy sand soils; sod weakly-podzolic sandy loam soils; sod mainly gleyed sandy, loamy-sandy and sandy soils with humous sands soils	loam-sandy	4.5-5.0 very strong acidic	mixed	0.00163 high
KYR	6.8± 3.44	157± 14.7	sod medium-podzolic loamy sand soils	sandy-loam	4.5-5.0 very strong acidic	broadleaved	0.0004 moderetly high
NYV	4.1± 2.81	181± 10.1	sod medium-podzolic loamy sand soils	sandy-loam	4.5-5.0 very strong acidic	broadleaved	0.0004 moderetly high
DUB	4.8± 3.39	161± 12.4	sod medium-podzolic loamy sand soils	sandy-loam	4.5-5.0 very strong acidic	broadleaved	0.0004 moderetly high

Table S2

Comparison of linear mixed-effects models with different combinations of ring width predictors based on AIC Values

Model	df	AIC
Null Model (random effect)	3	994.49
age + soil mechanical composition	4	**799.3173**
age + soil type	6	989.07
age + forest type	4	982.75
age + pH	4	986.42
age + altitude	4	985.4
age + slope	4	985.95
soil type + soil mechanical composition	5	804.86
soil type + forest type	6	990.07
soil type + pH	5	992.6
soil typeand altitude	6	990.22
soil type + slope	6	991.86
age + soil mechanical composition + pH	4	799.3173
age + soil mechanical composition + altitude	5	**799.3089**
age + soil mechanical composition + slope	5	800.2733
age + soil mechanical composition+ forest type	4	799.3173

According to the results of the MANOVA test, adding any additional third component to a model already incorporating age and soil mechanical composition does not result in a statistically significant improvement in the model's explanatory power or efficiency.

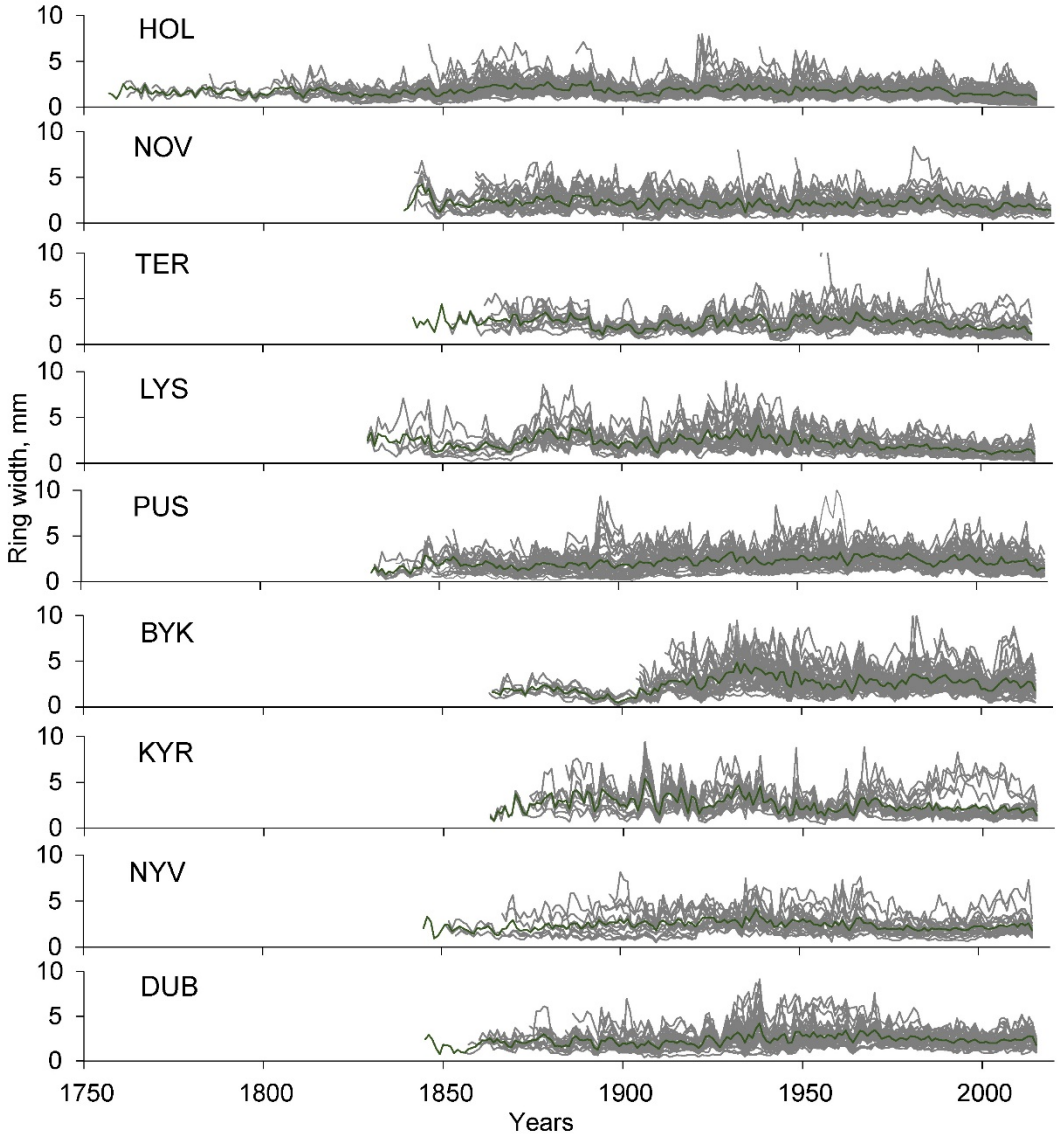

Fig. S1. Raw chronologies for each study site (see Table 1 for site ID code meaning)

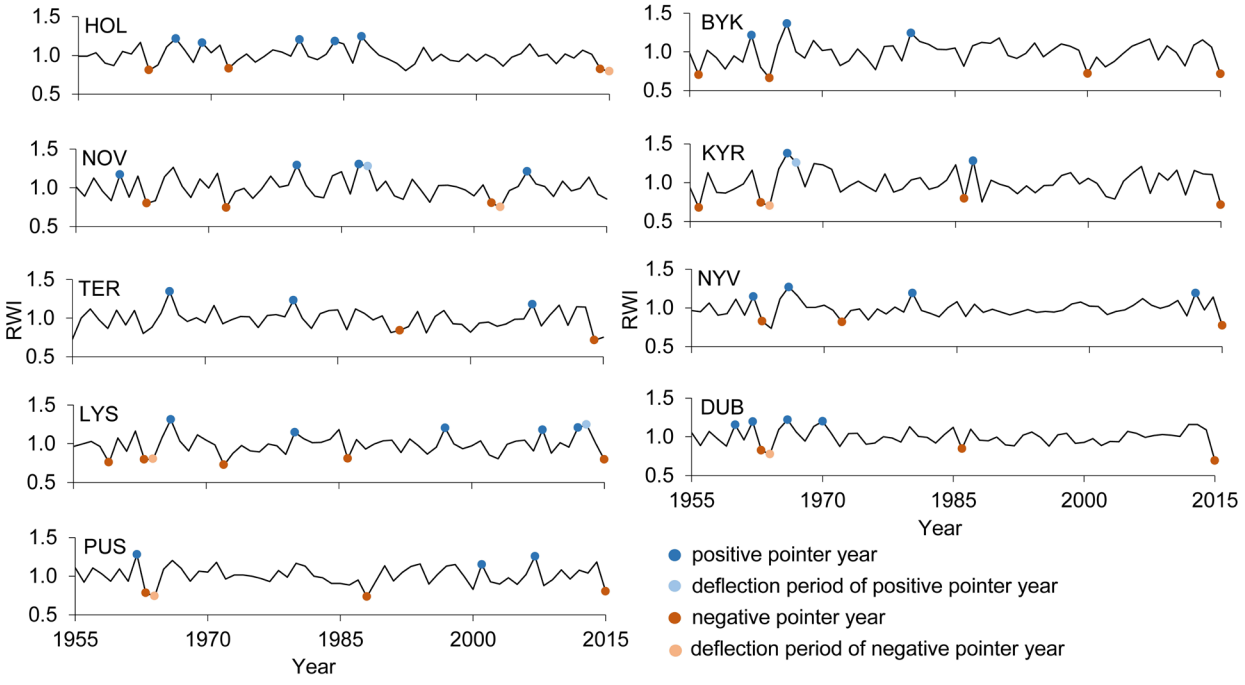

Fig. S2. The negative and positive pointer years with the following deflection period detected by the BSGC method

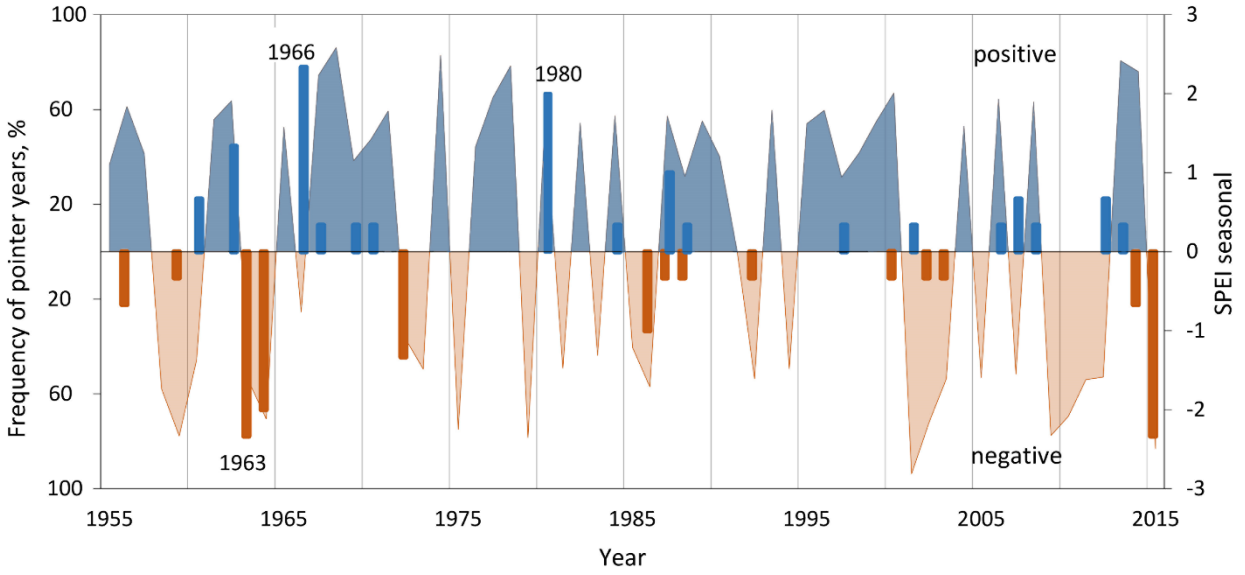

Fig. S3. The negative and positive pointer years frequency throughout studied forests (bars) and values of minimum and maximum seasonal SPEI indices, i.e. from April to September (shaded area)

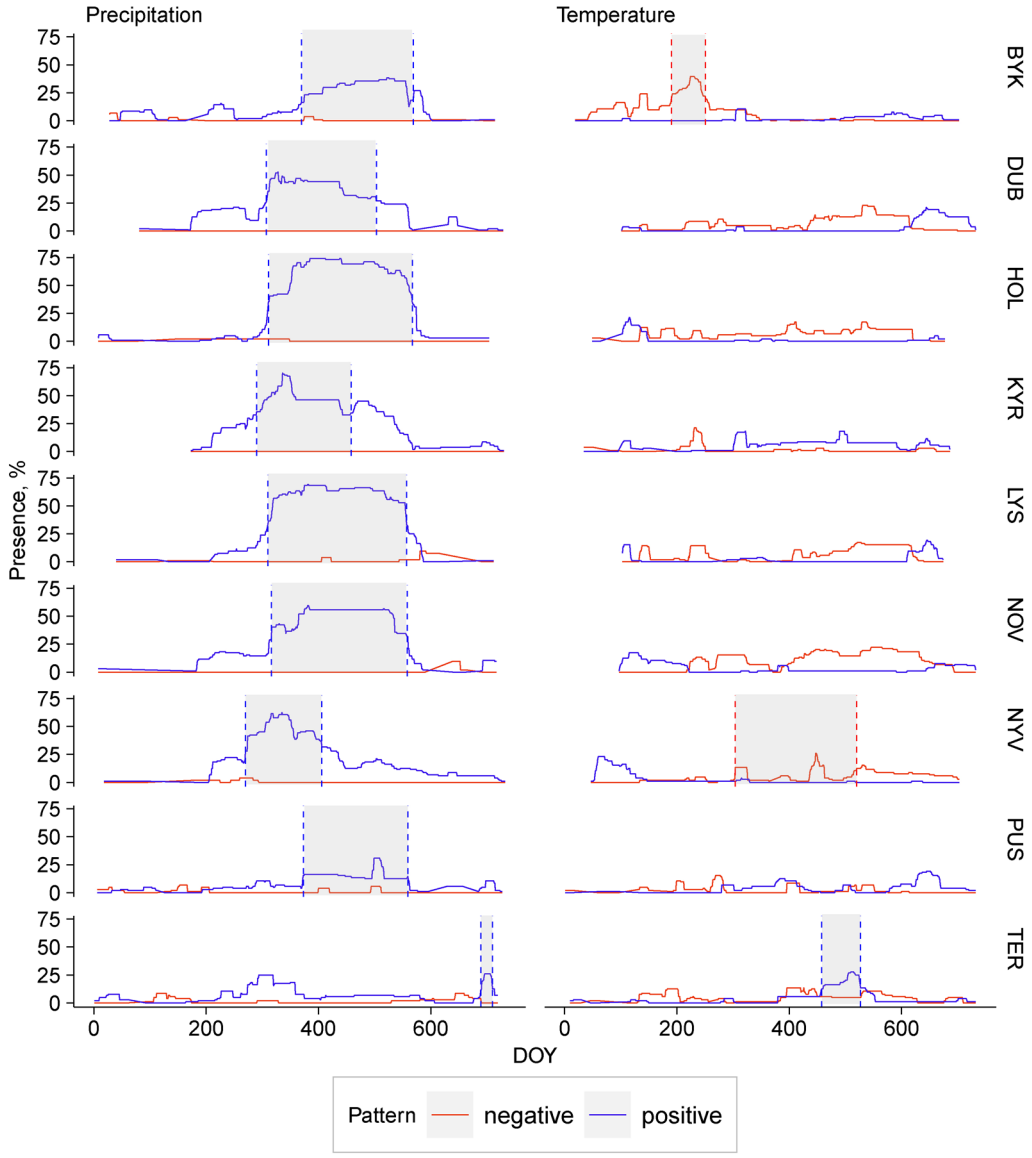

Fig. S4. The presence (%) of each day of a dendrochronological year (DOY) in the most influential patterns of the climate-to-growth relationships occurred in the 104 matrices of 31-yr consecutive time-windows from 1882 to 2015 (see Fig. 3). Shaded areas highlight the full duration at half maximum (FDHM) obtained from the presence distribution's peak exceeded the threshold of 25 %

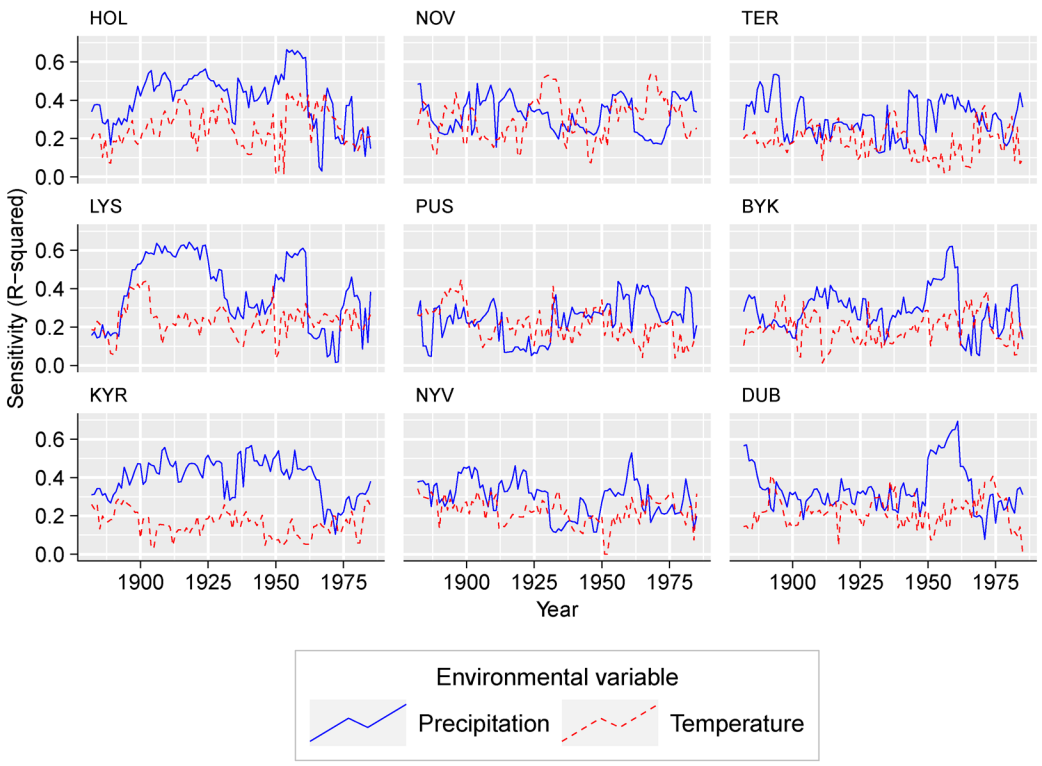

Fig. S5. Line graph presenting changes of trees' climatic sensitivity extracted as R-squared from a simple linear model with RWI as a response variable and temperature or precipitation as the predictors. Climatic variables were aggregated into optimal sequences for each time window